Harmonic distortion reduction on seismic vibrators

Zhouhong Wei and Thomas F. Phillips, ION Geophysical Corporation

To improve seismic resolution using vibroseis, vibrators must output the ground-force energy with minimum harmonic distortion. Four main sources within the vibrator system cause the ground force to suffer severe harmonic distortion: the nonlinear servo-valve flow-pressure characteristics, the servo-valve characteristics near null, the fluctuations in the hydraulic pressure, and the nonlinear contact-stiffness between the baseplate and the ground. Modeling was undertaken to investigate and quantify harmonic distortion from each source. As a result, three modifications have been made to reduce the harmonic distortion of the ground force:

- The hydraulic power system was changed to suppress ripples on the hydraulic pressure.
- The baseplate was stiffened.
- Nonlinear control algorithms to reduce low-frequency harmonics produced by the servo-valve system were implemented.

Experimental results demonstrate that these changes dramatically reduce the harmonic distortion in the ground-force signal under various coupling conditions, particularly on hard and uneven ground.

Introduction

With conventional vibrators, due to nonlinear effects in the hydraulic system and the low rigidity of the baseplate, harmonic distortion is generated as the ground force is exerted by the baseplate. These harmonics in the raw recorded data result in trains of correlated noise, known as harmonic ghosts, in the correlated data. The second and third harmonics account for most of this distortion (Walker, 1995; Polom, 1997).

If the harmonic ghosts can be eliminated completely, the energy output could be increased, resulting in better signal-to-noise ratio. Improving the ability of the vibrator to output ground force with less harmonic distortion has become a key factor in modern vibrator design. Due to servo-valve nonlinear flow-pressure characteristics and servo-valve characteristics near null, the servo-valve assembly on the vibrator produces significant harmonics dominated by the third and the fifth harmonics (Garagić and Srinivasan, 2004). Because of the nonlinearity in the servo-valve assembly, the hydraulic power supply creates huge ripples rich in the second and the fourth harmonics. Meanwhile, due to the low rigidity of the baseplate, the nonlinear contact-stiffness between the baseplate and the ground creates additional challenges. It is difficult, on highly variable surface conditions, such as desert sand dunes, to achieve good coupling, and vibrating on these surfaces generates more harmonic distortion. Rocking and flexing also take place on the baseplate as well, causing poor repeatability of source signatures and inaccurate measurement of the actual ground force.

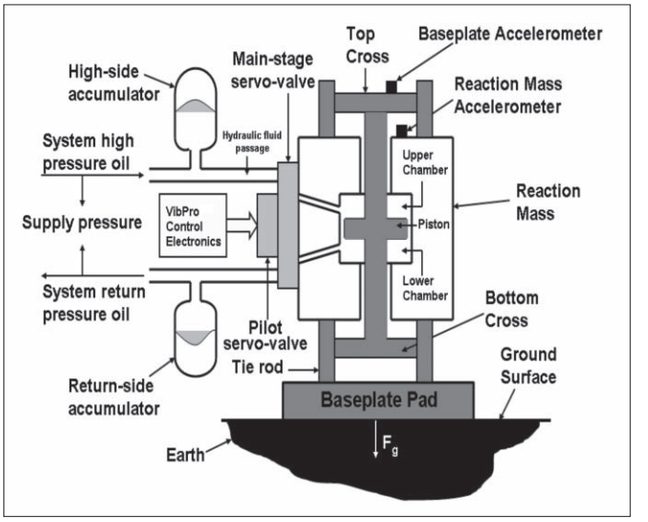

Figure 1. *Schematic of an AHV-IV vibrator.*

A modern seismic vibrator is essentially a hydro-mechanical system driven by a servo-valve assembly controlled electronically. Figure 1 shows a cross section of an ION AHV-IV vibrator. Hydraulic pressure powers the servo-valve assembly which consists of a pilot servo-valve and a main-stage servo-valve. With the preload system (PLS), the piston, the top and bottom crosses, and four tie rods and tubes are firmly connected to form a stilt structure where the reaction mass sits. This stilt structure is mechanically joined with the baseplate pad. The piston moves in a cylindrical bore inside the reaction mass and divides the cylinder into an upper and lower chamber. The control electronics outputs sweep signals as commands to drive the servo-valve assembly which then feeds the high-pressure hydraulic oil alternately into the upper and lower chambers to drive the reaction mass up and down. The force acting on the reaction mass is equally and oppositely applied to the piston. Through the baseplate-driven structure, the force is transmitted into the ground.

Sallas (1984) presented a weighted-sum method to approximate the ground force (F_g) by summing weighted baseplate and reaction mass accelerations as shown in Equation 1. For an AHV-IV vibrator, the baseplate and reaction mass accelerometers are mounted on the top cross and the top of the reaction mass, respectively.

$$-F_g = M_r A_r + M_b A_b \qquad (1)$$

In Equation 1, M_r, M_b, A_r, and A_b stand for the mass of the reaction mass, the mass of the baseplate, the reaction mass acceleration, and the baseplate acceleration. The weighted-sum method assumes the baseplate is a rigid body. However, for the vibrator baseplate, the rigid body assumption is true only below 50 Hz. Because of the flexure of the baseplate pad and very complicated rocking of the baseplate stilt structure, placing the baseplate accelerometer in different locations

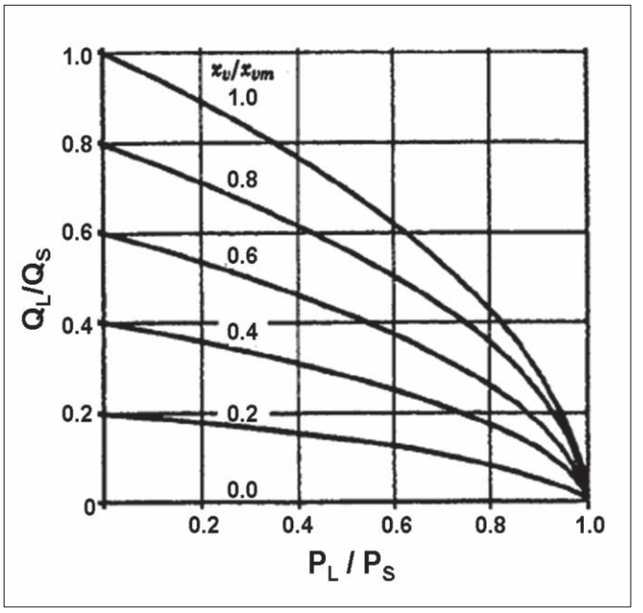

Figure 2. *Change in the load flow with the valve displacement and the load pressure.*

within the baseplate will generally produce different dynamic motion records. This means that the weighted-sum method can approximate the ground force only in a narrow frequency bandwidth.

Servo-valve nonlinearity

Electro-hydraulic servomechanisms are used in many industrial applications because of their high power-to-weight ratio, high stiffness, and high payload capability. The servo-valve assembly is powered by the supply pressure which is the difference between the system high pressure and the system return pressure. The dynamic characteristics of the servo-valve assembly are dominated by the dynamics of the main-stage servo-valve which is governed by a nonlinear equation that relates the load pressure (P_L) and supply pressure (P_s) to flow rate of the hydraulic oil (Q_L) as shown in Equation 2 (Merritt, 1967). K, defined as an orifice flow coefficient, is constant and X_V is the servo displacement. In addition, Equation 2 shows that the load flow is proportional to the servo-valve displacement, meaning that the nonlinear square-root relationship can be scaled by the valve displacement: the larger the servo-valve displacement, the stronger the nonlinearity.

Figure 2 is plotted in a normalized manner to further demonstrate this nonlinearity. The horizontal axis is the load pressure normalized to the supply pressure while the vertical axis is the load flow normalized to the supply flow (Q_S). Curves are plotted at different levels of the servo-valve displacement which is normalized to the maximum servo-valve displacement (X_{VM}). The maximum servo-valve displacement is defined as the maximum distance physically available for the servo-valve spool to travel. The curves are labeled 0.0, 0.2, 0.4, 0.6, 0.8, and 1.0 to correspond to servo-valve displacements of 0, 20, 40, 60, 80, and 100% of the maximum servo-valve displacement. Figure 2 shows that the load flow

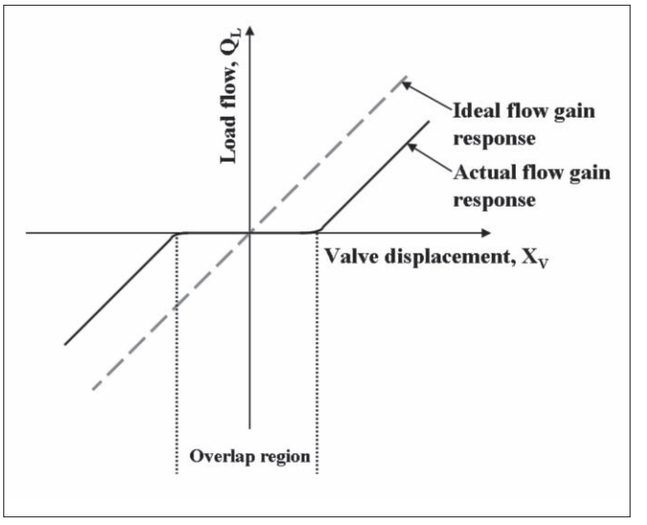

Figure 3. *Load flow gain and overlap of the main-stage valve.*

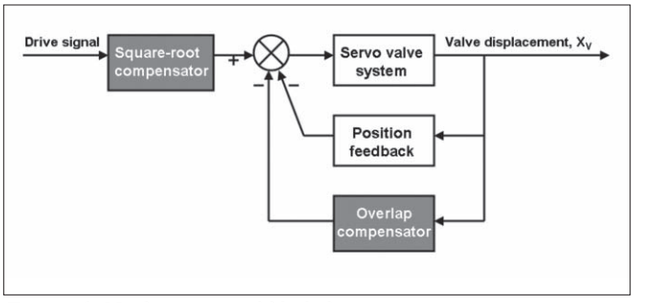

Figure 4. *Nonlinear control block diagram.*

and the load pressure are related in a nonlinear manner at any level of servo-valve displacement. This nonlinear square-root causes significant harmonics to appear in the load pressure. Ultimately, these harmonics show up as harmonic distortion noise in the ground force.

$$Q_L = KX_V \sqrt{P_s - \frac{X_V}{|X_V|} P_L} \qquad (2)$$

Another source of nonlinearity, the "zero lap" cut, occurs because the spool used to close the gap in the servo-valve is usually machined to have an overlap to prevent loss of fluid pressure. For the Atlas 240 H main-stage servo-valve, the overlap is approximately 1.5% of the servo-valve maximum displacement (0.254 cm).

Figure 3 exhibits a flow gain response to the main-stage servo-valve spool displacement. Ideal flow gain response, a straight line through the origin, would exist if an ideal "zero lap" cut of the main-stage servo-valve spool could be manufactured. Thus, an overlap region or a dead band is created in the flow gain response. This causes a nonlinear flow gain response to the main-stage servo-valve displacement and, therefore, harmonics during the main-stage servo-valve movement.

These two sources of nonlinearity and undesirable harmonics can be attenuated using nonlinear control algorithms

Integration of Pelton DR-valve technology and nonlinear control algorithms

The Pelton DR-valve, mounted between the pilot servo-valve and the main-stage servo-valve, causes the output of a vibrator to track the desired reference input more closely. The DR valve converts the main-stage servo-valve from a flow-control type of servo-valve into a pressure-control type of servo-valve (Reust, 1993). With the DR valve, the feedback control of the vibrator ground force outputs small control variables to smoothly correct the amplitude and phase in the fundamental frequency, resulting in more accurate control of the vibrator. This smooth and accurate control of the fundamental component in the vibrator ground force increases the vibrator response to uncertainties in the system. In addition, the baseplate and Earth resonance is damped, reducing harmonic distortion.

Nonlinear control algorithms compensate for the nonlinear behavior of the main-stage servo-valve. These control algorithms linearize the square-root and overlap nonlinearities in the servo-valve system and reduce harmonics generated by the servo-valve system at low frequencies. Figure 4 shows the implementation of these nonlinear controls. The nonlinear square-root compensator relies on the exact cancellation of the square-root terms and the overlap compensator performs a negative feedback of the slope of the flow gain. These nonlinear compensators are programmed as software and embedded in control electronics.

Testing of the nonlinear control compensators was done with an AHV-IV model 362 vibrator on load cells (Wei, 2009). The vibrator is equipped with weights of 3654 kg (8120 lbs) and 1809 kg (4020 lbs) for the reaction mass and the baseplate, respectively. Figure 5 shows frequency-time plots of the ground force with the nonlinear control on and off. The vibrator performs a 10-Hz and 5-s linear sweep and shakes at 70% drive force. Figure 5a is plotted with the nonlinear control off and Figure 5b with it on. All harmonics are significantly reduced except the second, which is enhanced about 2 dB with the nonlinear control on. Overall, there is about 61% reduction on harmonic distortion with the nonlinear control. Figure 6 compares the ground force measured by load cells with nonlinear control compensators on and off. The data were recorded using a 10-s linear sweep from 1 to 21 Hz. Just as in Figure 5b, the second harmonic in Figure 6b increased as well. However, in general, Figure 6 demonstrates that nonlinear control techniques reduced harmonic distortion by roughly 36%.

Fluctuations of the hydraulic pressure

Typically, a hydraulic power supply system consists of pumps, a prime mover or a diesel engine to drive the pumps, a reservoir of fluid, a pressure regulator, relief valves for safety purposes, hydraulic filters, an oil cooler, and accumulators. Since the motion of the servo-valve is electronically controlled, the servo-valve displacement will follow the command input precisely. Most of the time, a sinusoidal sweep is output from the control electronics and the servo-valve displacement tracks this sinusoidal sweep. This sinusoidal load flow results

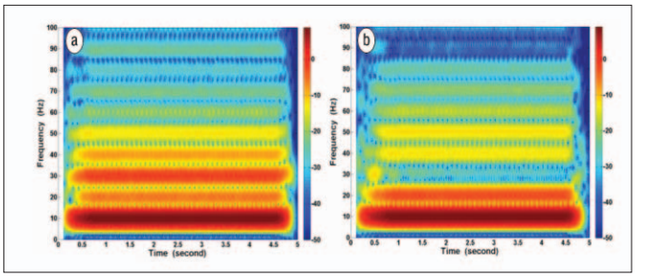

Figure 5. *Comparisons of the ground force measured by load cells. (a) Nonlinear control off. (b) Nonlinear control on.*

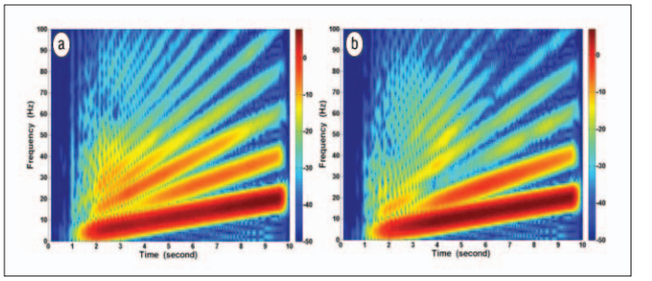

Figure 6. *Comparisons of the ground force measured by load cells at frequencies of 1–21 Hz. (a) Nonlinear control off. (b) Nonlinear control on.*

in a supply flow that looks very much like a rectified sine wave that is rich in the second harmonic. Because the pump is generally some distance from the main-stage servo-valve inlet, hoses and passageways pose a high-impedance path between the pump and load. This passage acts much like an inductor in an electrical circuit and tends to isolate the pump-pressure output from the main-stage servo-valve inlet when the flow fluctuates, generating ripples in the supply pressure at the main-stage servo-valve inlet. Accumulators are usually near the servo-valve to mitigate the problem. Hydraulic accumulators are often used to filter pressure pulsations from pumps, to filter pressure ripples from servo-valves, and to provide additional fluid under pressure to accommodate peak flow demands. These filters can reduce the harmonic distortion in the supply pressure. Unfortunately, in many modern vibrator designs, at the frequencies of interest accumulators are too far away from the point of use to be effective. In addition, high-frequency pressure spikes are created by a fluid hammer effect as the servo-valve switches through null and are reflected back into the supply and return pressure. These spikes are often so large that cavitations occur that can cause pitting of the servo-valve and other components.

Supply pressure harmonics directly affect the load flow that in turn contaminates the load pressure. Equation 2 shows the interdependence that exists between supply pressure and load pressure. Harmonics in the supply will corrupt the actuator pressure. This "unhealthy" loop can cause very high flow turbulence that can lead to an audible buzz in the servo-valve system and, eventually, the ground-force signal becomes distorted.

To overcome these hydraulic supply pressure fluctuations, a new supply pressure system was designed with shorter sup-

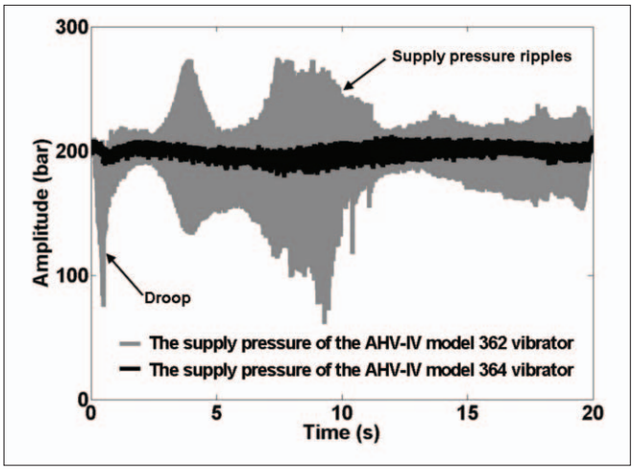

Figure 7. *The hydraulic supply pressures of the AHV-IV vibrators.*

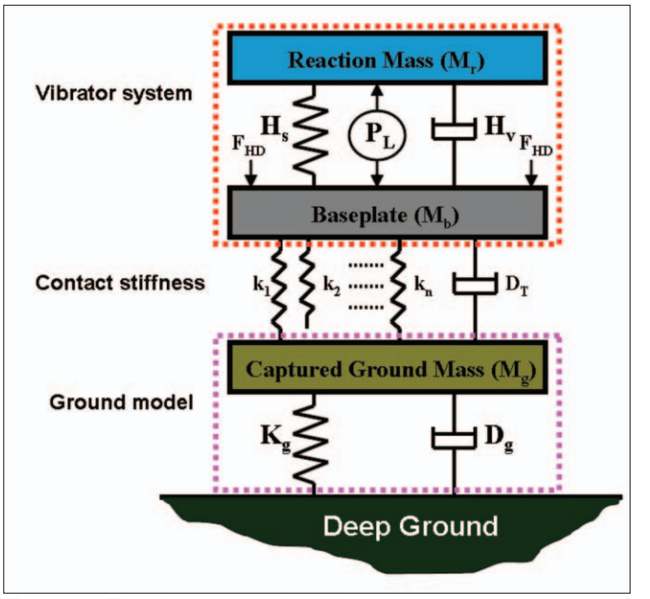

Figure 8. *The vibrator-ground model.*

ply lines and improved accumulators. This new supply pressure system is the result of a complete redesign of the hydraulic fluid flow hoses, accumulators, and flow passages in the reaction mass, and so on. The new design positions accumulators where they can be most effective and sizes passageways so that they are not restrictive.

In many instances, the surface of the ground is uneven and not fully coupled with the baseplate as the vibrator shakes. These uneven loadings cause large changes in flow demand throughout a sweep cycle as the servo-valve proportionally meters and redirects flow into the actuator. Peak flow demand generally ranges from 0 to 250 gallons per minute (gpm) at low frequencies within a cycle. Cyclical changes in flow demand can create huge supply pressure ripples rich in even harmonics and dominated by the second harmonic. This ripple effectively modulates the flow output of the main-stage valve, creating harmonic distortion in the differential pressure across the piston in the reaction mass chamber. This distorted differential pressure gives rise to distorted reaction mass and baseplate accelerations. Eventually, the ground force calculated by using the weighted-sum method is distorted by harmonics.

Figure 7 compares the supply pressures on vibrators with and without the redesign on a 20-s linear sweep from 5 to 105 Hz. Model 364 has the new actuator; model 362 carries the current production actuator. This figure documents the dramatic reduction in supply pressure ripples and initial "droop." Near the initiation of the sweep, the droop in the supply pressure has been reduced to almost a third of its previous magnitude. Figure 7 also shows that ripples throughout the sweep have been virtually eliminated. Ripples are evidenced by the large oscillations in the supply pressure of the vibrator with the old design. Also noteworthy is the improvement that was measured in ground force stability at high frequencies.

Contact stiffness and stiffer baseplate

Figure 8 depicts a simple vibrator-ground model. The vibrator can be simply described as the reaction mass connecting to the baseplate through the stiffness (H_S) and viscosity (H_V) of the hydraulic oil. Because the hydraulic oil can be assumed uncompressible in sweep frequency ranges and the friction of the hydraulic oil in the reaction mass chamber is very small, the stiffness and viscosity of the hydraulic oil do not impact dynamic forces produced by the reaction mass and the baseplate. The differential pressure or load pressure (P_L) is equally and oppositely applied to the reaction mass and the baseplate. In operation, the baseplate is coupled with the ground by applying a hold-down weight (F_{HD}) on the baseplate pad. The coupling of the baseplate and the ground significantly impacts vibrator performance. In general, the coupling conditions of the ground loaded to the baseplate have three variants. The first is determined by the captured ground mass (M_g), the ground stiffness (K_g), and the ground viscosity (D_g). This captured ground mass, also called the radiation mass, can be described as the ground mass participating in the motion caused by the ground force. The captured ground mass interacts with the deep ground through the ground stiffness and the ground viscosity. Very often, the ground stiffness changes during the vibrator's cycle of compressing and releasing the ground. However, the variation of the ground stiffness remains small and causes insignificant harmonics on the ground-force signal. The second variant of the coupling of the ground loaded to the baseplate is a product of the coupling media. Frequently, other media on top of the ground (e.g., loose gravel or sand) create harsh loading conditions and degrade the coupling. The roughness and unevenness of the coupling media lead to changeable contact areas between the baseplate and the ground. However, the changeable contact-stiffness caused by the coupling media is not a dominant fact that causes severe even harmonics. It is maximally effective only when the baseplate does not have sufficient stiffness. The third variant of the coupling conditions is the stiffness of the baseplate. When the vibrator shakes, the baseplate is subject to flexural vibrations due to

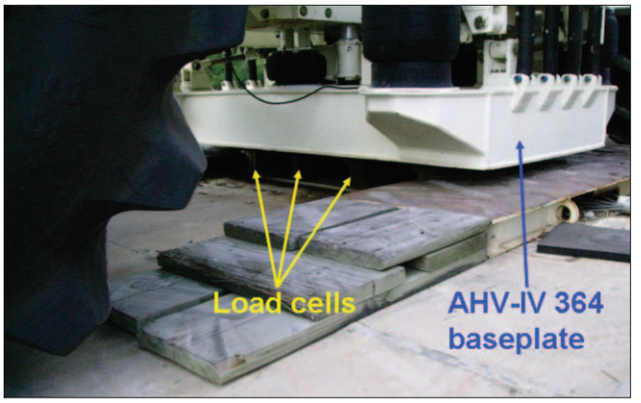

Figure 9. *Model 364 on load cells.*

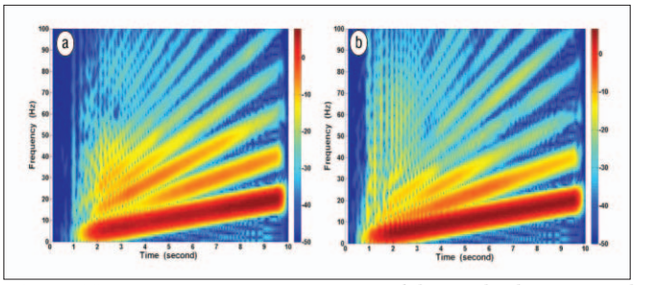

Figure 10. *Frequency-time representation of the weighted-sum ground force from 1–21 Hz. (a) Model 362. (b) Model 364.*

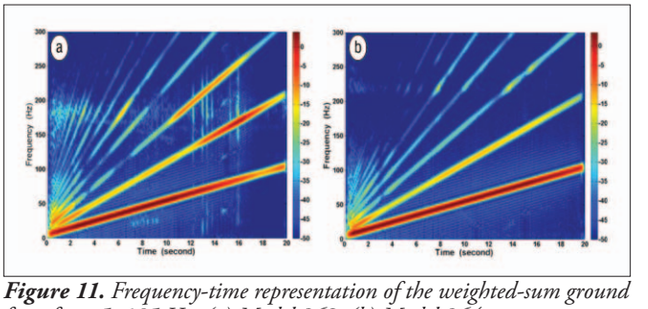

Figure 11. *Frequency-time representation of the weighted-sum ground force from 5–105 Hz. (a) Model 362. (b) Model 364.*

its low rigidity. As the sweep frequency goes up, the baseplate suffers severe flexure and complex rocking motions. In general, the contact area becomes larger when the baseplate is in its compressing ground cycle. The large contact area increases the contact stiffness. The contact area decreases when the baseplate is in the releasing ground cycle. The less contact area leads to small contact stiffness. Often, the coupling media exacerbate the asymmetry of the contact stiffness and this asymmetrical contact-stiffness is the dominant reason for rich even harmonics on the ground-force signal. Theoretically, stiffening the baseplate reduces its flexural vibration. Therefore, fewer variable values are in the contact stiffness. Subsequently, less harmonic distortion is seen in the ground force. As illustrated in Figure 8, the contact stiffness can be depicted as many springs in between the ground and the baseplate. Some springs fully connect the ground and the baseplate while others just make a single connection to either the ground or the baseplate or no connection at all. During operation, the spring disconnection to the baseplate and the ground becomes so severe that partial decoupling often occurs. Sometimes, full decoupling happens.

To improve coupling and maintain approximately constant stiffness between the ground and baseplate, one solution is to increase the hold-down weight of the vibrator. When a heavier hold-down weight is applied, the baseplate is pushed down more and the coupling media are squeezed to make more contact to the baseplate. More contact areas lead to less variation in stiffness. Another solution is to stiffen the baseplate (Wei, 2008). The most important benefit is enabling the best estimation of the true ground force by using the weighted-sum method in a broad frequency range (Wei, 2009). In turn, this allows a mass-spring-dashpot mechanical model to be good enough to describe the Earth response in that frequency band. The useful information of the Earth properties such as ground stiffness, ground viscosity, and coupled-ground mass can be retrieved correctly (Safar, 1984; Ley et al., 2006).

Experimental results

Figure 9 shows one test example with model 364 on load cells. This vibrator has a new modified hydraulic system, a new stiffer baseplate, and embedded nonlinear control compensators. A standard vibrator (model 362) used for data comparison did not have nonlinear control compensators. The Pelton DR-valve is on both. Eight load cells are evenly distributed in two rows under the baseplate, four in the front row and four in the back. All are firmly mounted on the concrete. A small rubber pad is inserted in between each individual load cell and the baseplate to protect the cells from metal-to-metal contact. Under these conditions, the baseplate is well coupled with the cells but the contact area is small. Severe decoupling exists between the baseplate and the concrete. The flexural vibration and complex rocking of the baseplate are severe. In the following frequency-time plots, the weighted-sum ground force is used for data comparison. The main reason for using the weighted-sum instead of the true ground force measured by load-cell sensors is that no vibrators are equipped with load-cell sensors in actual vibroseis acquisition. Another reason is that the weighted-sum ground force from model 364 has been proved to closely represent the true vibrator output (Wei, 2009; Hall, 2009).

Figure 10 is the frequency-time plot of weighted-sum ground forces using the standard model 362 vibrator and the new model 364. A 10-s linear sweep from 1 to 21 Hz was used to run both vibrators at a drive force of 70%. The Pelton DR-valve was turned on. Model 362 operated without nonlinear controls. Model 364 operated with nonlinear controls. A dramatic reduction in harmonic distortion at low frequencies was measured on the latter. There is a slight, 2 dB, enhancement on the second harmonic distortion from 4 to 6 s, corresponding to frequencies of 9–13 Hz. Reduction in harmonic distortion was pronounced. Furthermore, there were improvements in the uniformity, consistency, and intensity of the fundamental force with model 364. As documented in Figure 10, each harmonic shows a reduction in intensity. The

harmonics above the second were especially responsive to the design changes and the nonlinear controls.

Figure 11 shows another frequency-time plot of weighted-sum ground forces. Data were recorded using a 20-s linear sweep from 5 to 105 Hz. Both vibrators operated at a force level of 70%. The attributes of the frequency-time plots of the harmonic distortion on weighted-sum ground forces are quite similar to Figure 10. Overall uniformity, consistency and intensity of the fundamental force are greatly improved. Even more encouraging, the harmonic distortion is significantly reduced throughout the whole frequency range. Again, there is a reduction in the magnitude of each individual harmonic and, in particular, the overall noise at the low and high ends of the sweep is compensated for nicely. The second and third harmonics show a dramatic reduction.

Conclusions

Changes in vibrator design produced measurable improvement in the quality of the output signal and nonlinear controls suppressed harmonics in the weighted-sum ground force. When the vibrator is equipped with nonlinear controls, a pronounced reduction in the harmonic distortion is measured in the weighted-sum ground-force signal. Nonlinear control compensators using the Pelton DR-valve enable the vibrator to achieve low harmonic distortion at high force output over the entire sweep frequency band, especially at low frequencies. TLE

References

Garagić, D. and K. Srinivasan, 2004, Application of nonlinear adaptive control techniques to an electrohydraulic velocity servomechanism, *IEEE Transactions on Control System Technology*, 303–314.

Hall, M., 2009, Analysis of field tests with an improved hydraulic vibrator, SEG *Expanded Abstracts*, 104–108.

Ley, R., W. Adolfs, R. Bridle, M. Al-Homaili, A. Vesnaver, and P. Ras, 2006, Ground viscosity and stiffness measurements for near surface seismic velocity, *Geophysical Prospecting*, 751–762.

Merritt, H., *Hydraulic Control Systems*, 1967, Wiley.

Polom, U., 1997, Elimination of source-generated noise from correlated vibroseis data (the "ghost-sweep" problem), *Geophysical Prospecting*, 571–591.

Reust, D., 1993, Enhanced servovalve technology for seismic vibrators, *Geophysical Prospecting*, 43–60.

Sallas, J., 1984, Seismic vibrator control and the downgoing P-wave, Geophysics, 732–40.

Safar, M., 1984, On the determination of the downgoing P-wave radiated by the vertical seismic vibrator, *Geophysical Prospecting*, 392–405.

Walker, D., 1995, Harmonic resonance structure and chaotic dynamics in the earth-vibrator system, *Geophysical Prospecting*, 487–508.

Wei, Z., 2008, Reducing harmonic distortion on vibrators–stiffening the vibrator baseplate, EAGE *Extended Abstracts,* B006.

Wei, Z., 2009, How good is the weighted-sum estimate of the vibrator ground force?, *The Leading Edge*, 960–965.

Corresponding author: john.wei@iongeo.com